phys. stat. sol. (a) **126**, 151 (1991)

Subject classification: 71.55 and 73.40; 72.50; S5.11

Department of Physics, Technical University of Transport and Communication, Žilina[1])

Acoustic Deep-Level Transient Spectroscopy of MIS Structures

By

P. BURY, I. JAMNICKÝ, and J. ĎURČEK

A new method of determining and characterization of traps at the insulator–semiconductor interface is presented. This method, acoustic deep-level transient spectroscopy (A-DLTS), is based on the acoustoelectric response effect observed at the interface. A theoretical analysis of the acoustoelectric transient measurements in accordance to capacitance ones is also presented. The temperature dependence of the acoustoelectric response after bias voltage step application is investigated and the activation energies are calculated. Some other parameters of interface traps are also determined. The method is verified by the investigation of both, n- and p-type SiO_2–Si interface states.

Eine neue Methode zur Charakterisierung der Traps in der Grenzschicht von MIS-Strukturen wird vorgestellt. Diese Methode, akustische-DLTS genannt (A-DLTS), besteht in der Beobachtung der akustoelektrischen Response an der Grenzschicht. Eine theoretische Analyse der akustoelektrischen Transientenmessungen erfolgt in Beziehung zu ähnlichen kapazitiven Messungen. Die Abhängigkeit der akustoelektrischen Response wird nach sprunghafter Änderung der Vorspannung untersucht, und die Aktivierungsenergien werden berechnet. Einige andere Parameter der Traps in der Grenzschicht werden ebenfalls bestimmt. Die Methode wird durch die Untersuchungen an n- und p-leitenden SiO_2–Si-Grenzschichten überprüft.

1. Introduction

The interface states in metal–insulator–semiconductor (MIS) structures have been extensively studied for more than twenty years and many useful experimental methods have been developed to characterize them [1 to 6]. Among the more important methods are several modifications of the deep-level transient spectroscopy (DLTS) originally developed in 1974 [7] which investigate the response of an MIS structure to an applied voltage step [8 to 10].

In this paper we present a new modification of such spectroscopic method that enables to extend a number of DLTS techniques and can be also used in the cases, which are not easily accessible to previous techniques. We call this new technique acoustic deep-level transient spectroscopy (A-DLTS). The basic idea of this high-frequency ultrasonic method consists in the analysis of the acoustoelectric response of the MIS structure after bias voltage steps applied to the structure at various temperatures. Recently, we have found [11, 12] that the acoustoelectric signal produced by MIS structures, when a longitudinal acoustic wave propagates along them, strongly depends on the bias voltage applied to the structure and the acoustoelectric response behaviour reflects the changes in the space charge distribution in the interface region.

[1]) CS-01026 Žilina, Czechoslovakia.

2. Theory

The basic idea of A-DLTS presented here is connected, similarly to some other DLTS techniques, with the fact that the time development of the capacitance properties of semiconductor structures after applied bias voltage step reflects relaxation processes in the charge distribution in both the semiconductor volume and the interface layer. It is known [13] that a MIS structure propagated by an ultrasound wave produces an acoustoelectric signal like a capacitance transducer, the response of which can be expressed by the relative change of capacitance and accumulated charge. The relative change of the capacitance can be directly given by the relative deformation which in the case of a thin planar structure ($d \ll \lambda$) can be expressed by the ratio of pressure and elastic moduli. Thus, the amplitude of the acoustoelectric response can be written in the form

$$U_{ac} = U_i \frac{p_0}{K_i} + U_s \frac{p_0}{K_s} = \frac{Q}{C_i} \frac{p_0}{K_i} \left(1 + \frac{C_i}{C_s} \frac{K_i}{K_s}\right), \tag{1}$$

where U_i and U_s are the voltages on the insulator and the equivalent semiconductor capacitance, respectively, p_0 is the acoustic pressure amplitude, K_i, K_s and C_i, C_s are the elastic moduli and capacitances of insulator and semiconductor, respectively, and Q is the accumulated charge. Taking into account that $K_i \approx K_s$, U_{ac} can be expressed in the simplified form

$$U_{ac} = \frac{Q}{C} \frac{p_0}{K_i}, \tag{1a}$$

where

$$C = \frac{C_i C_s}{C_i + C_s} = \frac{C_i}{1 + C_i/C_s}$$

is the total capacitance of the structure.

By analyzing (1a) one can see that the change of amplitude U_{ac} can be caused by the change of accumulated charge Q or total capacitance C. So at constant Q only the time dependence of C_s can contribute to a transient signal occurring when the MIS structure charge distribution returns to an equilibrium state. The total capacitance C varies only in the case when C_i is larger than or comparable with C_s. However, in the real circuit (Fig. 1) the

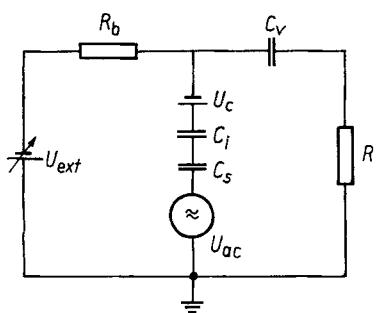

Fig. 1. The principal circuit of MIS capacitor in the experimental configuration as an acoustoelectric signal generator

structure is loaded by the receiver input impedance and it is necessary then to ensure the fulfilment of the condition $\omega RC > 1$, where R is the input resistance of the receiver and ω the ultrasound angular frequency. In the experimental arrangement this can be created by using a high impedance input receiver. Then the time development of received acoustoelectric signal reflects the time development of $1/Q$ that is used in the transient conductance or capacitance techniques as a starting point for the spectroscopic analysis.

In the case of thicker insulator layers ($\gtrsim 1$ μm), the value of the ratio C_i/C_s is small so that C remains constant and after the previous procedure one could not wait for any transient response. But in real cases the strong transient signals are observed under appropriate external conditions, the following explanation can be provided.

If the resistor R_b complies with the condition that the constant R_bC_i is smaller than the charge relaxation phenomena occuring in the structure, but still larger than the period of the ultrasound wave, the case with constant Q can no longer be considered. Taking into account that $C \approx C_i$, the acoustoelectric signal time dependence is given by

$$U_{ac}(t) = \frac{\int_0^t (I - I')\,dt}{C_i} \frac{p_0}{K_i}, \tag{2}$$

where the current I represents the contributions of non-delayed free charges and I' the delayed capture or emission processes which try to establish the equilibrium state and work against the bias voltage step, respectively. The current I is given by

$$I = \frac{U_b}{R_b} e^{-\frac{t}{R_bC_i}} \tag{3}$$

and the current I' can be expressed, for instance, through the capture mechanism in the form

$$I' = qN_t \frac{\partial f}{\partial t}, \tag{4}$$

where q is the electronic charge, U_b the bias voltage step, N_t the trap density, and f the distribution function of interface trap level occupancy. By substituting I and I' from (3) and (4) into (2), one can obtain the following formula:

$$U_{ac}(t) = \frac{U_bC_i(1 - e^{-\frac{t}{R_bC_i}}) - qN_t[f(t) - f(0)]}{C_i} \frac{p_0}{K_i}. \tag{5}$$

Considering only one kind of mechanism, $f(t)$ can be simply written in the form

$$f(t) = f_0(1 - e^{-\frac{t}{\tau}}), \tag{6}$$

where $f(t) = \pm [f(U + \Delta U) - f(U)]$, with positive or negative sign for emission or capture, respectively, $\tau = 1/e$ is the reciprocal value of capture or emission rate. Choosing R_b to comply with the condition $R_bC \ll \tau$, the acoustoelectric response signal is

$$U_{ac}(t) = \frac{U_bC_i - qN_tf_0(1 - e^{-\frac{t}{\tau}})}{C_i} \frac{p_0}{K_i}. \tag{7}$$

The considered arrangement is similar to that of the charge DLTS technique. The insulator and receiver input capacitances work as integrating elements. However, in some structures overlapping processes with different relaxation times can occur. These processes can be distinguished from the temperature or bias voltage dependence of the acoustoelectric response.

The relaxation time τ can be calculated from the recorded $U_{ac}(t)$ using any other appropriate numerical technique. The reciprocal value of τ gives the emission rate which for electrons is given by the relation

$$e_n = \frac{1}{\tau_n} = \sigma_n \langle v_{th} \rangle N_c \, e^{-\frac{\Delta E}{kT}}, \tag{8}$$

where σ_n is the capture cross section, $\langle v_{th} \rangle$ the mean thermal velocity, N_c the effective density of states at the bottom of the conduction band, and ΔE the trap activation energy related to the bottom of the conductivity band. Replacing $\langle v_{th} \rangle$ and N_c by the adequate formulae

$$\langle v_{th} \rangle = \left(\frac{3kT}{m_n^x} \right)^{1/2}, \qquad N_c = \frac{1}{4} \left(\frac{2m_{hn} kT}{\pi \hbar^2} \right)^{3/2},$$

we obtain for the case of electrons

$$\tau_n^{-1} = \gamma_n \sigma_n T^2 \, e^{-\frac{\Delta E}{kT}}, \tag{9}$$

where

$$\gamma_n = \frac{2^{5/2} 3^{1/2} \pi^{3/2} k^2 m_{hn}^{*3/2}}{h^3 m_n^{*1/2}}$$

Here $m_{hn}^* = (m_n^* m_h^*)^{1/2}$, where m_n^*, m_h^* is the effective mass of electrons and holes, respectively. Similar relations can be found also for the hole emission or capture processes. In this case the density of states at the valence band edge should be taken into account and the calculated energy values are related to the valence band edge. Then the trap cross sections $\sigma_{n,p}$ and the activation energies ΔE can be determined from the logarithmic dependence of τT^2 on $1/T$. However, there exist temperature dependences of σ, γ, and ΔE which are neglected by this procedure. Therefore, the determined values of $\sigma_{n,p}$ and ΔE are called apparent cross section and apparent activation energy, but they are frequently used for the identification of traps.

The analysis of the time dependence of the acoustoelectric signal also allows to determine the trap concentration. According to (7) the ratio of signal height at the time $t \to \infty$, that means in the new stationary state, to the signal height at $t = 0$, that means that instantaneously before the bias voltage is applied, is given by

$$x = \frac{U_{ac}(t \to \infty)}{U_{ac}(t = 0)} = \frac{U_b - \dfrac{qN_t f_0}{C_i}}{U_b}$$

and for the number of occupied states we have

$$N_t f_0(t) = \frac{U_b C_i (1 - x)}{q} \tag{10}$$

In the case when the total capacitance of the structure varies with time (thin oxide layer) the problem becomes non-linear and can be solved only approximately. However, the experimental results show that the exponential character of the acoustoelectric signal development remains by fulfilling the condition $R_b C(t) \ll \tau$ for the whole period of measurement. This development follows then the relaxation time of the charge transfer.

3. Experimental Procedure

The acoustoelectric response measurement arrangement for MIS and other structures is illustrated in Fig. 2. The investigated structure was acoustically bonded to the quartz rod buffer, on the other side of which the longitudinal acoustic wave, mostly of frequency 4.6 MHz, was generated by a $LiNbO_3$ transducer driven by a Matec attenuation comparator. The MIS structure worked as a receiver transducer. The acoustoelectric signal from the structure after detection in the receiver was selected and averaged by the box-car integrator and could be recorded as a time function by both the analogous–digital converter coupled to a personal computer and by the recorder. The external bias voltage was applied to the investigated structure through the resistor R_b. The capacitor C_v protected the receiver input against dc voltage. The investigated structure together with buffer and transducer was situated in the brass holder placed in the nitrogen cryostat, which enabled the measurement of the temperature dependence of the acoustoelectric response.

The relaxation time range 10^{-3} to 10^{3} s could be covered in this way. The lower limit of the relaxation times is not inherent in the acoustic method but it is given by the repetition frequency of the used Matec attenuation comparator and can be at maximum 10 kHz. For times in the range 10^{-6} to 10^{-3} s a variant of the technique can be used utilizing the shape of the bias voltage pulse applied to the structure in various times before the acoustoelectric pulse signal is generated by the structure. A pulse generator with variable delay and pulse width must be used as a source of bias voltage pulses synchronically triggered with acoustic pulse generator. The dependence of the acoustoelectric signal amplitude on the time interval between the bias voltage and acoustic pulses is then measured.

The character of the observed processes can be determined starting from (7) and the following simple rule for the acoustoelectric response time development. If the charge carriers

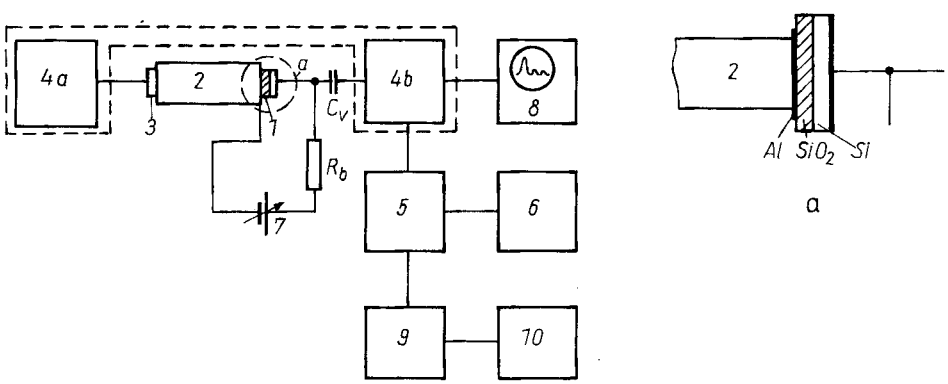

Fig. 2. Block diagram of acoustoelectric response measurement apparatus: 1 Si MIS structure, 2 buffer, 3 transducer, 4 Matec attenuation comparator, 5 box-car integrator, 6 recorder, 7 bias voltage supply, 8 oscilloscope, 9 analogous–digital converter, 10 computer. $f = 4.6$ MHz, $P_{ac} \approx 0.1$ to 1.0 W/cm^2

are negative, their emission and capture cause an increase and decrease of the acoustoelectric signal, respectively. In the case of the positive charge carriers and the same polarity the situation is opposite.

For the complete evaluation the measured parameters can be directly calculated from the experimental data logged in the computer memory without any graphical output. Nevertheless, graphical outputs at different steps of evaluation are recommended for surveying the correct experimental and evaluation procedures.

The well-known Si MOS structures were firstly investigated to verify the principles of the above-discussed method – acoustic DLTS. The Al–SiO_2–Si capacitors were fabricated both on n-type Si substrates with (100) surface orientation and 2.6 to 2.8 Ω cm resistivity and on p-type Si substrates with the same orientation and 8.0 to 8.7 Ω cm resistivity. The oxide layers were grown by CVD technique to two different thicknesses 80 and 800 nm. The phosphor silicate glass (PSG) was grown as an additional insulator layer of thickness 1180 nm, so that a 1980 nm thick layer was prepared, too. Aluminium was deposited onto the insulator layer using a vacuum evaporation. Oxide from the backside of the wafer was removed and Al or Ag was deposited to provide the back contacts. The detailed capacitor configuration is illustrated on the right-hand side of Fig. 2.

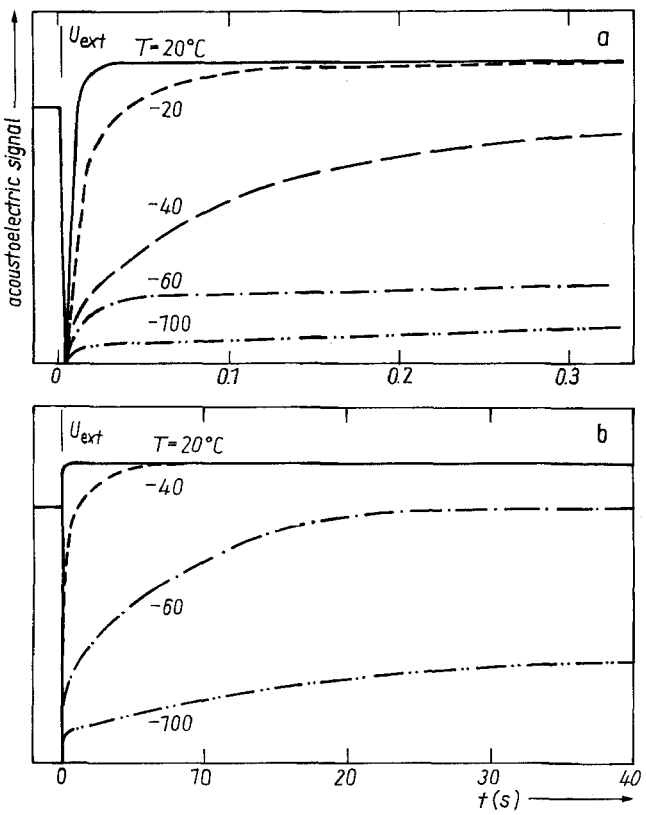

Fig. 3. Time development of acoustoelectric response at various temperatures and external bias voltage U_{ext} = 100 V registered by a) computer and b) recorder for the 800 nm thick oxide sample. The substrate was n-type, 2.6 Ω cm

4. Results and Discussion

Using the above-described technique the development of the acoustoelectric response signal as a function of temperature was investigated for all different MIS structures mentioned in the previous part. Fig. 3 shows the measured time dependence of acoustoelectric response of the Si MOS structure with an oxide layer thickness 800 nm prepared on n-type substrate for several temperatures. The increase of the relaxation time with decreasing temperature is clearly visible. The applied external voltage step was $U_{ext} = 100$ V starting from zero external field and had the polarity oriented against the contact potential U_c. Therefore, the acoustoelectric signal at first rapidly decreases to zero and then increases to the quasi-equilibrium state. In the structure it corresponds to the rapid response of free carriers connected with the creation of a depletion layer and relaxation processes strongly dependent on the temperature representing the examined transient effects, respectively. It should be noted that the required external voltage step value depends, except on the oxide thickness, also on the geometrical arrangement of the structure. While in our previous work [12] the buffer electrode ensured a perpendicular electric field all over the sample, in the present configuration (Fig. 2a) the smaller electrode on the oxide side deteriorates it so that a larger external field must be used. The sample configuration change was necessary because of the electric leakage effect at the sample edge. However, this change of the value of the external bias voltage step has no influence on the time development of the acoustoelectric response signal. However, the time dependence of the acoustoelectric response signal can be more complicated in the presence of more than one process.

Such dependences were observed for the Al–SiO_2–Si (n) structure with 80 nm thick oxide layer, where the temperature dependences of the acoustoelectric response signals (Fig. 4) enable to distinguish two processes with different relaxation times.

In the case of p-MOS structures only measurements on the structures with oxide thicknesses 1980 and 800 nm provide reliable results. The measurement on the structure with 80 nm thick oxide was impossible, probably because of the strong surface potential fluctuations [6]. The time development of the acoustoelectric response recorded at various

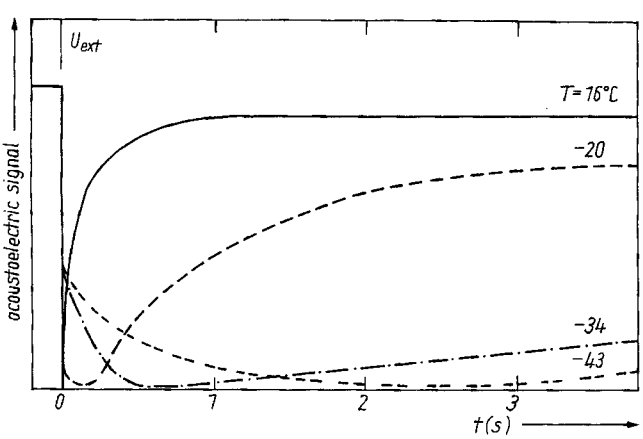

Fig. 4. Time development of acoustoelectric response at various temperatures and external bias voltage $U_{ext} = 8$ V registered by a computer for the 80 nm thick oxide sample. The substrate was n-type, 2.6 Ω cm

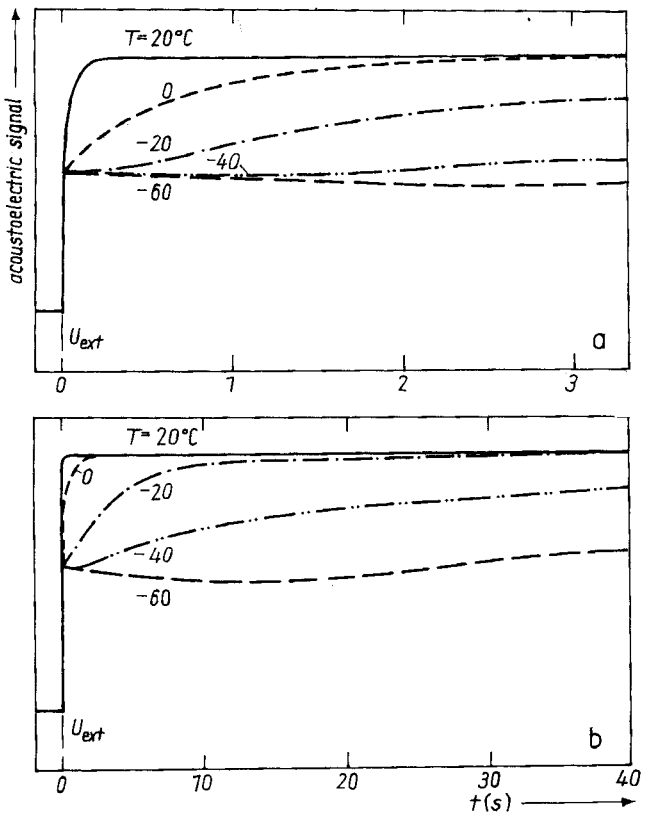

Fig. 5. Time development of acoustoelectric response at various temperatures and external bias voltage U_{ext} = 70 V registered by a) computer and b) recorder for the 800 nm thick oxide sample. The substrate was p-type, 8.7 Ω cm

temperatures for 800 nm thick oxide is shown in Fig. 5. It can be seen that there are again two mechanisms. The polarity of the external bias voltage was opposite to that of the n-MOS structures.

Using (9) and the above experimental curves of the acoustoelectric signal dependences partially shown in Fig. 3, 4, and 5, the Arrhenius plots for all measured structures could be constructed (Fig. 6). The resulting apparent activation energies found from these plots and the corresponding calculated apparent cross sections are summarized in Table 1 for measured structures. The character of processes and the number of occupied states at room temperatures calculated using (10) are given in Table 1, too.

Table 1

Summary of the trap parameters detected by the A-DLTS in Si-MOS structures

substrate	n ($N_d = 5 \times 10^{15}$ cm^{-3})			p ($N_a = 1 \times 10^{15}$ cm^{-3})	
d (nm)	800	80	80	800, 1980	800, 1980
ΔE (eV)	0.48	0.38	0.20	0.33	0.54
$\sigma_{n,p}$ (cm^2)	3.3×10^{-15}	6.0×10^{-19}	0.6×10^{-20}	2.1×10^{-20}	2.8×10^{-16}
N_t (cm^{-2})	1.3×10^{11}	1.1×10^{11}		4.5×10^{11}	
process	e-emiss.	e-emiss.	e-capture	h-emiss.	e-emiss.

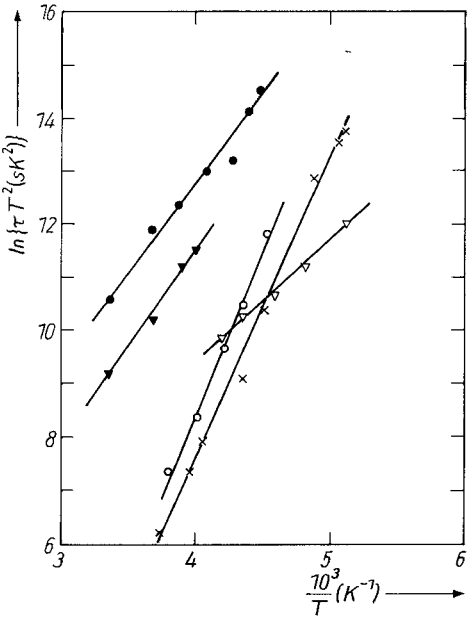

Fig. 6. Arrhenius plots constructed using (9) and the time dependences of acoustoelectric response partially illustrated in Fig. 3 (×), Fig. 4 (△, ▲), and Fig. 5 (○, ●). Full and open symbols were determined from the increasing and decreasing part of the acoustoelectric response signal, respectively

Most of the obtained energy levels are in good agreement with the values found by other techniques. The direct comparison with the capacitance DLTS technique is possible only in the case of the structure with thin (80 nm) insulator layer. However, the advantage of our method is connected with the possibility to measure also structures with thick oxide layer. In such cases small changes in the charge distribution cause large potential changes on the small capacitance of the dielectric layer. Thereby a comparison with similar capacitance or conductance techniques is not possible. In spite of this difference we have compared our results with some others observed by different techniques.

The obtained deep trap level near 0.48 eV below the conduction band edge was observed by various techniques and was determined as a donor level in the SiO_2–Si interface [14 to 17]. The energy level position at 0.38 eV below the conduction band edge is very close to the donor levels between 0.37 and 0.40 eV found by both DTLS and other techniques and associated with oxygen precipitates [18, 19] or with some kinds of defect formations [16, 17, 20, 21]. The third energy level obtained in the n-MOS structure at 0.20 eV above the valence band edge was rarely confirmed as an acceptor level [15], but as a donor level as well [22]. The energy level at 0.33 eV above the valence band edge found in the p-MOS structure coincide with the interface trap levels at 0.30 to 0.35 eV [6, 14, 15, 23] and/or some impurity levels in Si [20, 24]. The energy level position at 0.54 eV below the conduction band edge agrees with the values found using DTLS and other techniques for the bulk impurity [15, 20, 24 to 26] and some kinds of structural defects [18]. However, the interface states with continuous level distributions are reported mostly as results obtained by the conductance technique [6, 14, 16, 28]. These effects are eliminated from our results probably by the used evaluation technique and their weakness. We could observe them may be by a more careful analysis of the obtained curves, for instance, using the method of Fourier analysis. The measurements on the n-type MOS structures also indicate the influence of the oxide thickness on the obtained trap level positions.

The calculated cross sections are usually of the order of 10^{-16} cm^2 [6, 23, 24], but in our technique the sensitivity of the determined values on the external conditions as oxide thickness, energy level position, and used approximation is much larger than in the case of activation energy determination. Therefore, the direct comparison is difficult. However, cross sections several orders of magnitude smaller can be found in some references [17, 19,

26, 27], that coincide with our results. On the other hand, the determination of the trap densities is more precise because it is related directly to the measured changes of the acoustoelectric response signal. The determination of the volume concentrations remains uncertain because of the uncertainity of the depletion region thickness.

5. Conclusion

The acoustic-DLTS technique is introduced and analysed. The acoustoelectric response signal provoked by the ultrasound wave propagated through the MIS structure reflects the instantaneous situation in the charge relaxation caused by emission or capture processes. The emission or capture rate can be determined from the time development of this signal. From the temperature dependence of the time development of the acoustoelectric response signal the energy level positions of the traps and their emission or capture cross sections can be determined. The dependence of the acoustoelectric response signal on the polarity of the applied external voltage gives information about the charge of the transient carriers and the type of the trapping process. This new modification of the DLTS technique can also be used in the case of thick insulator layers, when the capacitance or admittance techniques are not convenient. At the same time, this procedure can be used also to describe other effects in the structure as, for instance, dielectric layer polarization or contact potential. It should be mentioned that an alternative acoustic-DLTS technique based on the measurement of the transverse electrical voltage provoked by surface acoustic waves has been proposed and discussed in [29 to 32]. It was called the transverse acoustic voltage spectroscopy.

Acknowledgement

The authors would like to express their gratitude to Dr. O. Mikuš for supplying the MIS structures.

References

[1] L. TERMAN, Solid State Electronics **5**, 285 (1962).
[2] E. H. NICOLLIAN, A. GOETZBERGER, and C. N. BERGLUND, Appl. Phys. Letters **15**, 174 (1969).
[3] D. R. YOUNG, E. A. IRENE DI MARIA, and R. F. DE KEERSMAECKER, J. appl. Phys. **50**, 6366 (1979).
[4] W. L. TSENG, J. appl. Phys. **62**, 591 (1987).
[5] K. PATER, Appl. Phys. A **44**, 191 (1987).
[6] K. K. HUNG and Y. C. CHENG, J. appl. Phys. **62**, 4204 (1987).
[7] D. V. LANG, J. appl. Phys. **45**, 3014 (1974).
[8] I. THURZO and J. JAKUBOVIE, J. Phys. D **14**, 1477 (1981).
[9] K. I. KIROV and K. B. RADEV, phys. stat. sol. (a) **63**, 711 (1981).
[10] M. SCHULZ and N. M. JOHNSON, Appl. Phys. Letters **31**, 622 (1977).
[11] P. BURY, J. ĎURČEK, and K. SAKALAUSKAS, phys. stat. sol. (a) **95**, K207 (1986).
[12] P. BURY, J. ĎURČEK, and O. MIKUŠ, Acta phys. Slov. **37**, 259 (1987).
[13] J. ĎURČEK and P. BURY, in: Proc. 7th Czech. Conf. Electronic and Vacuum Physics, Bratislava 1985 (p. 602).
[14] S. KAR and R. L. NARISMHMAN, J. appl. Phys. **61**, 5353 (1987).
[15] M. H. WHITE and J. R. CRICCHI, IEEE Trans. Electron Devices **19**, 1280 (1972).
[16] A. N. NAZAROV, V. S. LYSENKO, S. A. VALIEV, M. M. LOKSHIN, A. S. TKACHENKO, and I. A. KUNITSKII, phys. stat. sol. (a) **120**, 447 (1990).

[17] E. KAMIENIECKI and R. NITECKI, Proc. Internat. Topical Conf. The Physics of SiO_2 and Its Interface, Yorktown Heights (N.Y.) 1978 (p. 417).
[18] K. SCHMALZ, F.-G. KIRSCHT, and K. TITTELBACH-HELMRICH, phys. stat. sol. (a) **109**, 279 (1988).
[19] P. K. MCLARTY, J. W. COLE, K. F. GALLOWAY, D. E. IOANNOU, and S. E. BERNACKI, Appl. Phys. Letters **51**, 1078 (1987).
[20] Y. DAI, Solid State Electronics **32**, 439 (1989).
[21] E. F. DA SILVA, JR., Y. NISHIOKA, and T. P. MA, Appl. Phys. Letters **51**, 270 (1987).
[22] H. KITAGAWA and S. TANAKA, phys. stat. sol. (a) **120**, K67 (1990).
[23] F. HOFMANN and W. H. KRAUTSCHNEIDER, J. appl. Phys. **63**, 1358 (1989).
[24] V. PANDIAN and V. KUMAR, phys. stat. sol. (a) **109**, 273 (1988).
[25] S. J. VLASOV, S. Z. ZAINABIDONOV, J. N. KARIMOV, and A. A. NASIROV, Soviet Phys.–Semicond. **21**, 467 (1987).
[26] J. PROKEŠ and O. STEFAN, JR., phys. stat. sol. (a) **114**, 643 (1989).
[27] D. R. YOUNG, E. A. IRENE, D. J. DIMARIA, and R. F. DEKEEISMEAKER, J. appl. Phys. **50**, 6366 (1979).
[28] H. S. HADDARA and M. EL-SAYED, Solid State Electronics **31**, 1289 (1988).
[29] M. TABIB-AZAR, NAM-CHUN PARK, and P. DAS, Solid State Electronics **30**, 705 (1987).
[30] M. TABIB-AZAR, Solid State Electronics **31**, 1197 (1988).
[31] M. TABIB-AZAR and F. HAJJAR, IEEE Trans. Electron Devices **36**, 1189 (1989).
[32] P. KOŠTIAL, I. JAMNICKÝ, and J. ĎURČEK, phys. stat. sol. (a) **116**, K77 (1989).

(Received February 4, 1991; in revised form May 2, 1991)